Available online at www.sciencedirect.com

ScienceDirect

Mendeleev Commun., 2024, **34**, 242–245

Mendeleev Communications

Low-temperature synthesis in the dittmarite–sodium acetate trihydrate system: electrochemical activity of M^{3+}/M^{2+} redox couples in $AMPO_4$ (A = Na, Li; M = Mn, Mn/Fe)

Aleksandr Sh. Samarin,*[a] Tatiana V. Ivanova,[a,b] Eugene E. Nazarov,[a] Sergey N. Marshenya,[a] Nikita D. Luchinin,[a] Evgeny V. Antipov[a,c] and Stanislav S. Fedotov[a]

[a] *Skolkovo Institute of Science and Technology, 121205 Moscow, Russian Federation. E-mail: aleksandr.samarin@skoltech.ru, samarinchem@gmail.com*
[b] *D. I. Mendeleev University of Chemical Technology of Russia, 125047 Moscow, Russian Federation*
[c] *Department of Chemistry, M. V. Lomonosov Moscow State University, 119991 Moscow, Russian Federation*

DOI: 10.1016/j.mencom.2024.02.027

Phase-pure $NaMPO_4$ (M = Mn, Mn/Fe; isotypic to triphylite) and $Li(Mn/Fe)PO_4$ were isolated as a result of the low-temperature reaction between $NH_4MPO_4·H_2O$ (M = Mn, Mn/Fe) and $AcONa·3H_2O$ or AcOLi, respectively. Electrochemical tests in half-cells revealed that Na-based compounds exhibit poor electrochemical activity *vs*. metallic Na, while the similarly synthesized Li counterpart demonstrates decent cycling in Na cells. The synthetic features, crystal structures and properties of related members of the olivine family are discussed.

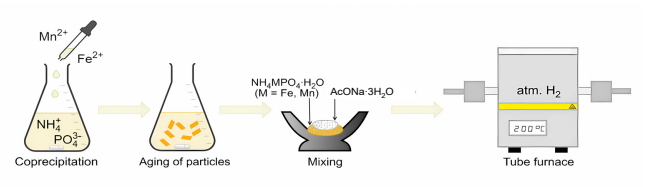

Keywords: topochemical reaction, olivine, triphylite, maricite, natrophilite, dittmarite, cathode material, battery, chimie douce.

Nowadays, sodium-ion batteries (SIBs) are considered a complement to the well-established lithium-ion technology. A number of different chemicals have been studied as the basis for designing and creating positive and negative electrode materials for SIBs.[1,2] Among them, compounds with oxoanions, mainly phosphates, such as $AMPO_4$ (A = Na, Li; M = Fe, Mn or a mixture thereof)[3] or $Na_3M_2(PO_4)_3$ (M = V, Mn, triple- or higher-charged cation or a mixture thereof),[4–8] have been the focus of many research groups over the past three decades.[9–11]

There are two known forms of compounds described by the formula $AMPO_4$ (M = Mn, Fe): maricite[12] and triphylite,[13–15] which both belong to the olivine family.[16,17] The electrochemical activity of maricite-structured phosphates and their carbon-enriched composites has been a matter of debate for at least a decade.[18] While maricite is the most stable form of $NaMPO_4$, Na-based counterparts of triphylite (in nature the mineral natrophilite $NaMnPO_4$) seem to be metastable, and their direct synthesis by high-temperature annealing is rather thermodynamically unfavorable.

Reported approaches to the synthesis of $NaMPO_4$ isotypic to $LiFePO_4$ can be classified into two groups. The first group includes a two-step ion-exchange reaction, involving the delithiation of $LiFePO_4$/C with subsequent Na insertion.[19] It is noteworthy that the introduction of Mn hinders the delithiation process (typically if the Mn content exceeds 60%).[20] The second group approach was pioneered by Lee *et al.* in 2011.[21] It was stated that the heat treatment of the dittmarite-structured precursor $NH_4MPO_4·H_2O$ (M is a doubly charged cation[22]) and a sodium salt, namely $AcONa·3H_2O$ (sodium acetate trihydrate), in the temperature range of 65–100 °C (the duration of the synthesis and other features of the procedure are not indicated in the original source) makes it possible to stabilize a wide range of phases of $NaMPO_4$ (M = Mn, Fe, $Fe_{0.5}Mn_{0.5}$, $Mg_{0.2}Mn_{0.8}$) phosphates[21] through the so-called topochemical reaction.[23]

At the moment, only a few works have been devoted to the preparation of $NaMPO_4$ by the above-mentioned topochemical route.[21,24,25] In this work, we addressed the possibility of stabilizing phase-pure $NaMnPO_4$ and $Na(Mn/Fe)PO_4$ in the $NH_4MPO_4·H_2O$ (M = Mn, Mn/Fe)–$AcONa·3H_2O$ systems. Additionally, the synthesis of $Li(Mn/Fe)PO_4$ was successfully performed. The resulting compounds were characterized by powder X-ray diffraction (XRD), Fourier-transform infrared spectroscopy (FTIR), thermogravimetric (TG) analysis, scanning electron microscopy (SEM) and energy-dispersive X-ray analysis (EDX). Electrochemical tests in half-cells revealed almost no electrochemical activity of Na-based compounds *vs.* metallic Na, while the similarly synthesized Li counterpart demonstrated decent cycling performance in the same cell type.

Taking into account previous studies of the $NH_4MnPO_4·H_2O$–$AcONa·3H_2O$[25] and $NH_4(Mn/Fe)PO_4·H_2O$–$AcONa·3H_2O$[24] systems, for the topochemical synthesis of $NaMPO_4$ (M = Mn, Mn/Fe) we used a 10-fold excess of sodium salt [Figure S3(*a*), see Online Supplementary Materials]. It was performed at 200 °C in a stream of pure H_2 for 12 h, followed by carbon coating at 410 °C to avoid the formation of unwanted maricite impurities.[26,27] According to XRD data, pure Mn and mixed (Mn/Fe) samples with carbon coating do not contain any traceable impurities [Figure 1(*a*),(*b*)]. Rietveld refinements were performed in the space group *Pnma* and confirmed that both $NaMnPO_4$ and $Na(Mn/Fe)PO_4$ (Tables 1, S1 and S2, see Online Supplementary Materials) are frameworks isotypic to the $LiFePO_4$ one.[24,28] The mixed Mn/Fe compound is characterized

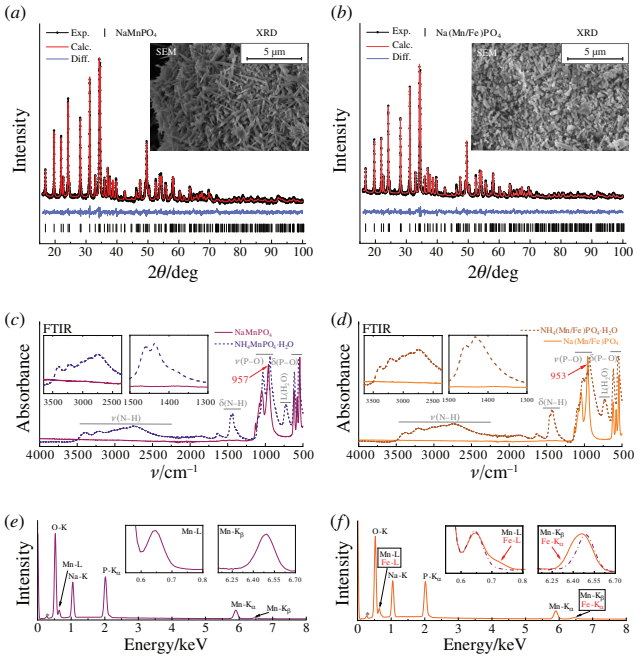

Figure 1 Experimental, calculated and difference XRD patterns of (*a*) $NaMnPO_4$/C and (*b*) Na(Mn/Fe)PO_4/C after Rietveld refinement. Bragg reflections are indicated by black bars. Insets: SEM images of (*a*) $NaMnPO_4$ and (*b*) Na(Mn/Fe)PO_4. FTIR spectra of (*c*) $NaMnPO_4$ and $NH_4MnPO_4{\cdot}H_2O$, as well as (*d*) Na(Mn/Fe)PO_4 and NH_4(Mn/Fe)$PO_4{\cdot}H_2O$ in the range of 4000–500 cm^{-1}. The insets show an enlarged region on stretching (left) and bending (right) vibrations of the NH_4^+ cation. SEM-EDX spectra of (*e*) $NaMnPO_4$/C and (*f*) Na(Mn/Fe)PO_4/C. The carbon line is indicated by *.

by slightly lower unit cell parameters, which suggests the formation of an Fe-substituted phase.[24] In $NaMnPO_4$, sodium ions are located in the M1 sites, forming zigzag chains of edge-sharing NaO_6 octahedra along the *b*-axis, similar to LiO_6 in $LiFePO_4$. In principle, this connectivity motif should give rise to 1D ion diffusion channels for sodium ions (Figure S1).

The completeness of the topochemical reactions was also confirmed by FTIR data [Figure 1(*c*),(*d*)]. In the FTIR spectra of both samples there are no characteristic bands corresponding to residual NH_4^+ cations or water. A slight decrease of vibration frequency from 957 to 953 cm^{-1} is additional evidence of the formation of an Fe-containing sample.[24,29] One can see a set of bands belonging to the O–P–O vibrations, stretching (1150–900 cm^{-1}) and bending (650–400 cm^{-1}), which remained practically unchanged. These observations are consistent with previous studies of the olivine crystal type.[24,30]

According to SEM data, the resulting powders consist of small thin plates of varying sizes from submicron to 5 μm in the greatest dimension and a thickness of about 200–400 nm. By analyzing the morphology of the Mn-containing material, a strong tendency to form needle-like particles could be noticed. The introduction of Fe into the crystal structure results in the formation of irregularly shaped particles with no discernible orientation. EDX measurements were carried out to verify the expected formula. For $NaMnPO_4$, the Na/Mn ratio was found to be very close to 1 : 1 [Figure 1(*e*),(*f*)]. EDX examination of the mixed phosphate demonstrates the presence of iron in the sample and the Na/Mn/Fe ratio is 1.01(1) : 0.87(9) : 0.11(2). For clarity, we denote the latter as Na(Mn/Fe)PO_4.

TG-DSC analysis reveals a decrease in the temperature of the transition to maricite. Thus, Na(Mn/Fe)PO_4 undergoes the phase transition at 605 °C and $NaMnPO_4$ at 625 °C (Figure S4). According to phase analysis data, both powders belong to the maricite crystal type with *V*(Mn/Fe) = 319.49(3) $Å^3$ and *V*(Mn) = 321.31(2) $Å^3$.[31,32] The decrease in unit cell volume *V* correlates with the presence of iron in the first sample

Table 1 Cell parameters for $NaMnPO_4$ and Na(Mn/Fe)PO_4 after Rietveld refinement.

Formula	$NaMnPO_4$	Na(Mn/Fe)PO_4
Space group	*Pnma*	
a/Å	10.5296(6)	10.4865(9)
b/Å	6.3471(3)	6.3281(5)
c/Å	4.9959(3)	4.9859(4)
V/$Å^3$	333.89(3)	330.86(5)
Z	4	
GOF	1.27	1.55
R_{exp} (%)	1.22	1.03
R_p (%)	1.22	1.19
R_{wp} (%)	1.55	1.60

[Figure S4(*b*)]. The IR spectra of maricites are consistent with published data.[33,34] Both peak regions, namely 1200–800 cm^{-1} and 650–540 cm^{-1}, are characteristic of stretching and bending vibrations of the PO_4 group, respectively. The difference in peaks position probably indicates different P–O bond lengths resulting from the substitution of Fe for Mn [Figure S4(*c*)]. The transition to the maricite phase leads to degradation of ion transport properties due to narrow migration channels unsuitable for the diffusion of alkali ions.[35–38]

Next, we performed electrochemical testing on Mn-rich $AMPO_4$ (A = Na, Li). The absence of noticeable electrochemical activity of natrophilite in sodium cells was previously shown by Boyadzhieva *et al.*[39] In Li half-cells, the carbon-enriched $NaMnPO_4$ composite exhibits rather modest performance.[40] As part of this work, we conducted a galvanostatic experiment on an iron-containing sample *vs.* metallic Na. Na(Mn/Fe)PO_4/C was cycled at the C/50 rate [Figure 2(*a*)]. However, no significant capacity was observed that could be explained by the reversible removal/insertion of Na ions. The shape of the curves and the

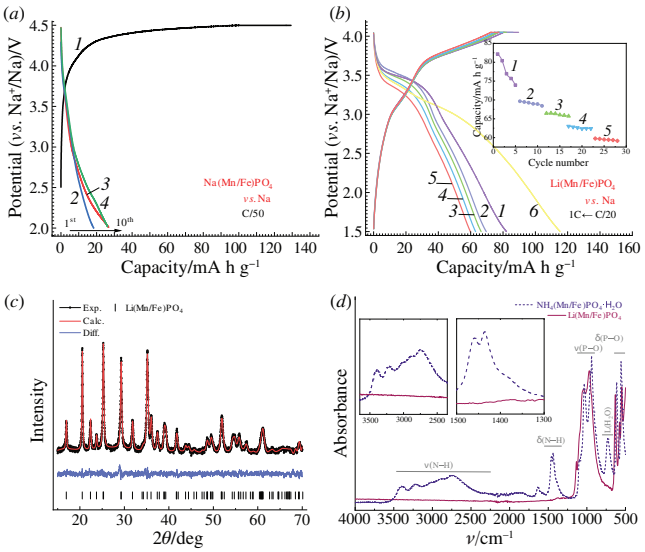

Figure 2 (*a*) Galvanostatic curves for (*1*) the 1st charge and the (*2*) 1st, (*3*) 5th and (*4*) 10th discharge, obtained in a two-electrode Na||Na(Mn/Fe)-PO_4 cell at the C/50 rate in the potential range of 2.0–4.5 V *vs.* Na^+/Na. (*b*) Galvanostatic charge/discharge curves obtained in a two-electrode Na||Li(Mn/Fe)PO_4 cell at the (*1*) C/20, (*2*) C/10, (*3*) C/5, (*4*) C/2 and (*5*) 1C rates in the potential range of 1.5–4.1 V *vs.* Na^+/Na. Yellow curve *6* corresponds to the 1st discharge process, *i.e.*, insertion of Na^+ ions. Inset: capacity *vs.* cycle number plots at the (*1*) C/20, (*2*) C/10, (*3*) C/5, (*4*) C/2 and (*5*) 1C rates. (*c*) Powder XRD pattern of Li(Mn/Fe)PO_4 with *a* = 10.3997(8) Å, *b* = 6.0742(4) Å, *c* = 4.7489(1) Å, *V* = 299.98(1) $Å^3$, space group *Pnma*, GOF = 1.30, R_p = 1.19 and R_{wp} = 1.51. (*d*) FTIR spectra of Li(Mn/Fe)PO_4 and NH_4(Mn/Fe)$PO_4{\cdot}H_2O$ in the range of 4000–500 cm^{-1}. The insets show enlarged regions of stretching (left) and bending (right) vibrations of the NH_4^+ cation.

discharge capacity values, not exceeding 25 mA h g^{-1}, suggest the capacitor type of behavior of this composite material.[41] Interestingly, some electrochemical activity of a similar mixed Mn/Fe-based composite was recently reported by Koleva *et al.*[24] However, those tests were conducted only on Li-half cells.

In contrast, Li-based mixed Mn/Fe triphylites are considered more viable hosts for sodium ions cycling.[42,43] The XRD pattern of the corresponding phosphate is shown in Figure 2(*c*). After the synthesis procedure, no traceable impurities were detected, and the cell parameters correspond to literature data.[44,45] The FTIR spectra [Figure 2(*d*)] confirm the results of the phase analysis. The absorption maxima can be attributed to the stretching and bending vibrations of O–P–O bonds, which is consistent with previous reports.[46–48] Additionally, the FTIR spectrum shows the absence of characteristic bands of –OH or H_2O.[27,46–51] The capacity during the first discharge, corresponding to the insertion of Na into the electrochemically delithiated framework [Figure 2(*b*), curve *6*], is prominently higher than that of subsequent discharges; the same feature had been observed by several groups previously.[19,20] The composite demonstrates reversible electrochemical cycling, exhibiting discharge capacities of 74 and 60 mA h g^{-1} at C/20 and 1C rates, respectively [Figure 2(*b*)]. In the galvanostatic charging curves, two distinct plateaus can be distinguished: the Fe^{3+}/Fe^{2+} reaction is observed near 3 V *vs.* Na^+/Na, and the Mn^{3+}/Mn^{2+} redox activity occurs at a higher potential of ~3.8 V *vs.* Na^+/Na. The observed values are within the same range as previously reported for a mixed composition with a Mn/Fe ratio of 4 : 1.[3,20,52]

In comparison to Fe-based counterparts such as $LiFePO_4$ or triphylite $NaFePO_4$,[53] Mn-rich phosphates demonstrate lower capacities and worse rate performance. This was observed during cycling in both Na- and Li-based electrolytes.[3,19,20] Experimental data on the chemical de-insertion of alkali metal cations also suggest that Mn-rich frameworks tend to retain a non-negligible residual amount of Li^+/Na^+ ions in the channels. For instance, Saurel *et al.*[20] mentioned that '$Fe_{0.2}Mn_{0.8}PO_4$ could not be fully delithiated, and as a result the sodiated sample is not single-phased' when continuously stirred with potassium persulfate $K_2S_2O_8$ in aqueous medium. The observed discharge capacities of '$Fe_{0.2}Mn_{0.8}PO_4$' and '$MnPO_4$' (~73 and ~58 mA h g^{-1}) confirm the assumption of incomplete delithiation. Only the use of quite aggressive oxidants in combination with special synthetic precautions makes it possible to stabilize phase-pure '$Fe_{0.2}Mn_{0.8}PO_4$'.[19] An additional reason for the significant hindrance of electrochemical activity is the peculiarity of the electronic structure of $NaMPO_4$ phosphates, in particular low electronic conductivity.[40] This is indirectly confirmed by the study of the optical absorption edge by UV-VIS spectroscopy, which allowed us to classify this form of $NaMPO_4$ as a wide bandgap insulator (the bandgap exceeds 5 eV).[54]

In this study, we successfully isolated phase-pure $NaMnPO_4$ and its mixed Mn/Fe counterpart using the corresponding dittmarites as precursors *via* a reaction under H_2 flow. The Rietveld refinement confirmed that the obtained Na-containing phosphates are isotypic to $LiFePO_4$. The results of the powder XRD data refinement are in agreement with the FTIR data. Both samples consist of small thin plates of varying sizes from submicron to 5 μm in the greatest dimension. For the first time, phase-pure mixed $Na(Mn/Fe)PO_4/C$ obtained under H_2 flow was tested in Na cells, however, no reversible electrochemical activity of the de/intercalation type was observed. At the same time, topochemically assisted synthesis allows the isolation of phase-pure mixed $Li(Mn/Fe)PO_4/C$, which exhibits reversible electrochemical cycling in Na-based cells. The chemical features of Mn-based triphylite counterparts were summarized and discussed. Further comprehensive study of this group of materials prepared by different synthetic routes is necessary to shed light on the observed sluggish electrochemical performance. The implementation of mild chemistry approaches as a tunable synthesis tool can provide enormous opportunities for the stabilization of various functional compounds.[55,56]

This work was supported by the Russian Science Foundation (project no. 17-73-30006). The authors are grateful to Center for Energy Science and Technology (Skoltech) graduate student Natalia Timusheva for assistance with SEM-EDX measurements and Dr. Sergey V. Ryazantsev for assistance with FTIR measurements and data processing. A.Sh.S. kindly thanks Prof. Olga V. Yakubovich and Dr. Galina V. Kiriukhina (Faculty of Geology, M. V. Lomonosov Moscow State University) for fruitful discussions. The authors also acknowledge the AICF of Skoltech for providing access to electron microscopy facilities.

Online Supplementary Materials

Supplementary data associated with this article can be found in the online version at doi: 10.1016/j.mencom.2024.02.027.

References

1 N. R. Khasanova, O. A. Drozhzhin, O. V. Yakubovich and E. V. Antipov, in *Comprehensive Inorganic Chemistry III*, 3rd edn., eds. J. Reedijk and K. R. Poeppelmeier, Elsevier, Amsterdam, 2023, vol. 7, pp. 363–403.
2 A. Sh. Samarin, I. A. Trussov and S. S. Fedotov, in *Comprehensive Inorganic Chemistry III*, 3rd edn., eds. J. Reedijk and K. R. Poeppelmeier, Elsevier, 2023, vol. 7, pp. 46–82.
3 B.-K. Zou, Y. Shao, Z.-Y. Qiang, J.-Y. Liao, Z.-F. Tang and C.-H. Chen, *J. Power Sources*, 2016, **336**, 231.
4 M. V. Zakharkin, O. A. Drozhzhin, I. V. Tereshchenko, D. Chernyshov, A. M. Abakumov, E. V. Antipov and K. J. Stevenson, *ACS Appl. Energy Mater.*, 2018, **1**, 5842.
5 M. V. Zakharkin, O. A. Drozhzhin, S. V. Ryazantsev, D. Chernyshov, M. A. Kirsanova, I. V. Mikheev, E. M. Pazhetnov, E. V. Antipov and K. J. Stevenson, *J. Power Sources*, 2020, **470**, 228231.
6 T. I. Perfilyeva, O. A. Drozhzhin, A. M. Alekseeva, M. V. Zakharkin, A. V. Mironov, I. V. Mikheev, Z. V. Bobyleva, A. P. Marenko, A. V. Marikutsa, A. M. Abakumov and E. V. Antipov, *J. Electrochem. Soc.*, 2021, **168**, 110550.
7 A. K. Ivanov-Shits and L. N. Dem'yanets, *Priroda* (*Nature*), 2003, no. 12, 35 (in Russian).
8 A. K. Ivanov-Shitz and V. V. Kireev, *Crystallogr. Rep.*, 2003, **48**, 112 (*Kristallografiya*, 2003, **48**, 117).
9 A. M. Abakumov, S. S. Fedotov, E. V. Antipov and J.-M. Tarascon, *Nat. Commun.*, 2020, **11**, 4976.
10 A. D. Dembitskiy, D. A. Aksyonov, A. M. Abakumov and S. S. Fedotov, *Solid State Ionics*, 2022, **374**, 115810.
11 S. S. Fedotov, A. Sh. Samarin and E. V. Antipov, *J. Power Sources*, 2020, **480**, 228840.
12 O. V. Yakubovich, E. L. Belokoneva, V. G. Tsirelson and V. S. Urusov, *Moscow Univ. Geol. Bull.*, 1992, **47** (6), 46 (*Vestn. Mosk. Univ., Ser. 4: Geol.*, 1992, no. 6, 54).
13 O. V. Yakubovich, M. A. Simonov and N. V. Belov, *Soviet Physics - Doklady*, 1977, **22**, 347 (*Dokl. Akad. Nauk SSSR*, 1977, **235**, 93).
14 O. V. Yakubovich, M. A. Simonov and O. K. Mel'nikov, *Soviet Physics - Crystallography*, 1990, **35**, 22 (*Kristallografiya*, 1990, **35**, 42).
15 V. A. Streltsov, E. L. Belokoneva, V. G. Tsirelson and N. K. Hansen, *Acta Crystallogr., Sect. B: Struct. Sci.*, 1993, **49**, 147.
16 L. Zhu, L. Li, J. Wen and Y.-R. Zeng, *J. Power Sources*, 2019, **438**, 227016.
17 O. Yakubovich, N. Khasanova and E. Antipov, *Minerals*, 2020, **10**, 524.
18 C. Berlanga, M. T. Sougrati, A. J. Fernández-Ropero, N. Baaboura, N. E. Drewett, J. M. Lopez del Amo, G. Nolis, J. S. Garitaonandia, M. Reynaud, L. Stievano, M. Casas-Cabanas and M. Galceran, *J. Mater. Chem. A*, 2023, **11**, 20506.
19 C. Henriksen, J. K. Mathiesen, Y.-M. Chiang, K. M. Ø. Jensen and D. B. Ravnsbæk, *ACS Appl. Energy Mater.*, 2019, **2**, 8060.
20 D. Saurel, M. Giner, M. Galceran, J. Rodríguez-Carvajal, M. Reynaud and M. Casas-Cabanas, *Electrochim. Acta*, 2022, **425**, 140650.
21 K. T. Lee, T. N. Ramesh, F. Nan, G. Botton and L. F. Nazar, *Chem. Mater.*, 2011, **23**, 3593.

22 G. V. Kiriukhina, O. V. Yakubovich and O. V. Dimitrova, *Crystallogr. Rep.*, 2015, **60**, 198 (*Kristallografiya*, 2015, **60**, 221).
23 C. Wu, J. Xie, G. Cao, X. Zhao and S. Zhang, *CrystEngComm*, 2014, **16**, 2239.
24 V. G. Koleva, T. J. Boyadzhieva and R. K. Stoyanova, *Cryst. Growth Des.*, 2019, **19**, 3744.
25 T. Boyadzhieva, V. Koleva and R. Stoyanova, *Bulg. Chem. Commun.*, 2013, **45** (Special Issue B), 208.
26 R. Tian, H. Liu, Y. Jiang, J. Chen, X. Tan, G. Liu, L. Zhang, X. Gu, Y. Guo, H. Wang, L. Sun and W. Chu, *ACS Appl. Mater. Interfaces*, 2015, **7**, 11377.
27 E. E. Nazarov, D. A. Aksyonov, E. V. Antipov and S. S. Fedotov, *Energies*, 2023, **16**, 5083.
28 M.-Y. Pan, S.-T. Lu, M.-Y. Zhang, C. Li, G.-D. Zou, K.-Z. Cao and Y. Fan, *J. Solid State Chem.*, 2023, **321**, 123929.
29 N. V. Kosova, A. B. Slobodyuk and O. A. Podgornova, *J. Struct. Chem.*, 2016, **57**, 345 (*Zh. Strukt. Khim.*, 2016, **57**, 359).
30 T. Boyadzhieva, V. Koleva and R. Stoyanova, *Phys. Chem. Chem. Phys.*, 2017, **19**, 12730.
31 V. Koleva, T. Boyadzhieva, E. Zhecheva, D. Nihtianova, S. Simova, G. Tyuliev and R. Stoyanova, *CrystEngComm*, 2013, **15**, 9080.
32 I. V. Korchemkin, I. V. Pet'kov, V. S. Kurazhkovskaya and E. Yu. Borovikova, *Russ. J. Inorg. Chem.*, 2015, **60**, 265 (*Zh. Neorg. Khim.*, 2015, **60**, 313).
33 T. Boyadzhieva, V. Koleva, P. Markov and R. Stoyanova, *Dalton Trans.*, 2021, **50**, 16548.
34 P. Venkatachalam, S. Ganesan, S. Rengapillai and S. Marimuthu, *Ind. Eng. Chem. Res.*, 2021, **60**, 5861.
35 P. P. Prosini, C. Cento, A. Masci and M. Carewska, *Solid State Ionics*, 2014, **263**, 1.
36 D. A. Aksyonov, S. S. Fedotov, K. J. Stevenson and A. Zhugayevych, *Comput. Mater. Sci.*, 2018, **154**, 449.
37 D. A. Aksyonov, A. O. Boev, S. S. Fedotov and A. M. Abakumov, *Solid State Ionics*, 2023, **393**, 116170.
38 N. V. Kosova, V. R. Podugolnikov, E. T. Devyatkina and A. B. Slobodyuk, *Mater. Res. Bull.*, 2014, **60**, 849.
39 T. Boyadzhieva, V. Koleva, R. Kukeva, D. Nihtianova, S. Harizanova and R. Stoyanova, *RSC Adv.*, 2020, **10**, 29051.
40 T. Boyadzhieva, V. Koleva, E. Zhecheva, D. Nihtianova, L. Mihaylov and R. Stoyanova, *RSC Adv.*, 2015, **5**, 87694.
41 S. Fleischmann, J. B. Mitchell, R. Wang, C. Zhan, D. Jiang, V. Presser and V. Augustyn, *Chem. Rev.*, 2020, **120**, 6738.
42 C. Heubner, T. Lein, M. Schneider and A. Michaelis, *J. Mater. Chem. A*, 2020, **8**, 16854.
43 C. Heubner, S. Heiden, M. Schneider and A. Michaelis, *Electrochim. Acta*, 2017, **233**, 78.
44 J. Schoiber, G. Tippelt, G. J. Redhammer, C. Yada, O. Dolotko, R. J. F. Berger and N. Hüsing, *Cryst. Growth Des.*, 2015, **15**, 4213.
45 V. A. Alyoshin, E. A. Pleshakov, H. Ehrenberg and D. Mikhailova, *J. Phys. Chem. C*, 2014, **118**, 17426.
46 E. E. Nazarov, A. D. Dembitskiy, I. A. Trussov, O. A. Tyablikov, I. S. Glazkova, A. V. Sobolev, I. A. Presniakov, I. V. Mikheev, A. V. Morozov, V. A. Nikitina, A. M. Abakumov, E. V. Antipov and S. S. Fedotov, *Energy Adv.*, 2023, **2**, 328.
47 E. E. Nazarov, O. A. Tyablikov, V. A. Nikitina, E. V. Antipov and S. S. Fedotov, *Applied Nano*, 2023, **4**, 25.
48 D. A. Aksyonov, I. Varlamova, I. A. Trussov, A. A. Savina, A. Senyshyn, K. J. Stevenson, A. M. Abakumov, A. Zhugayevych and S. S. Fedotov, *Inorg. Chem.*, 2021, **60**, 5497.
49 M. A. Kirsanova, S. V. Ryazantsev and A. M. Abakumov, *J. Solid State Chem.*, 2020, **286**, 121294.
50 V. D. Sumanov, D. A. Aksyonov, O. A. Drozhzhin, I. Presniakov, A. V. Sobolev, I. Glazkova, A. A. Tsirlin, D. Rupasov, A. Senyshyn, I. V. Kolesnik, K. J. Stevenson, E. Antipov and A. M. Abakumov, *Chem. Mater.*, 2019, **31**, 5035.
51 O. A. Drozhzhin, A. V. Sobolev, V. D. Sumanov, I. S. Glazkova, D. A. Aksyonov, A. D. Grebenshchikova, O. A. Tyablikov, A. M. Alekseeva, I. V. Mikheev, I. Dovgaliuk, D. Chernyshov, K. J. Stevenson, I. A. Presniakov, A. M. Abakumov and E. V. Antipov, *J. Phys. Chem. C*, 2020, **124**, 126.
52 M. Giner, V. Roddatis, C. M. López and P. Kubiak, *J. Electrochem. Soc.*, 2016, **163**, A650.
53 C. Berlanga, I. Monterrubio, M. Armand, T. Rojo, M. Galceran and M. Casas-Cabanas, *ACS Sustainable Chem. Eng.*, 2020, **8**, 725.
54 S. Jana, G. Lingannan, M. Ishtiyak, G. Panigrahi, A. Sonachalam and J. Prakash, *Mater. Res. Bull.*, 2020, **126**, 110835.
55 S. D. Shraer, N. D. Luchinin, I. A. Trussov, D. A. Aksyonov, A. V. Morozov, S. V. Ryazantsev, A. R. Iarchuk, P. A. Morozova, V. A. Nikitina, K. J. Stevenson, E. V. Antipov, A. M. Abakumov and S. S. Fedotov, *Nat. Commun.*, 2022, **13**, 4097.
56 A. I. Komayko, S. D. Shraer, S. S. Fedotov and V. A. Nikitina, *ACS Appl. Mater. Interfaces*, 2023, **15**, 43767.

Received: 5th December 2023; Com. 23/7333